Original Article
Food Science and Technology
ISSN 0101-2061 (Print)
ISSN 1678-457X (Online)
DOI: https://doi.org/10.5327/fst.7523

Properties characterization of binary composite hydrogels of gellan gum and *Aloe vera* blended at different ratios, pH, and solid contents

Verónica Guadalupe HERNÁNDEZ-BRIONES[1], Raúl GONZÁLEZ-GARCÍA[1], Jaime David PÉREZ-MARTÍNEZ[1], Alicia GRAJALES-LAGUNES[1], Miguel ABUD-ARCHILA[2], Miguel Angel RUIZ-CABRERA[1,*]

Abstract

Composite hydrogels based on natural polymers with manufactured properties according to the desired application for the food industry are currently significant. Thus, this study aimed to study the association of low acyl gellan gum (LAGG) and *Aloe vera* gel (AVG) for composite hydrogel creation by controlling pH (1, 4, 7), solid content (0.25, 0.50, 0.75 w/v), and polymer ratio (66:33, 50:50, and 33:66 LAGG/AVG). Hydrogels were prepared by physical crosslinking, diluting the required amount of LAGG at 90 °C, followed by AVG at 60 °C, and storing at 4 °C. The study involved the analysis of zeta potential (ξ), water holding capacity (WHC), hardness, storage modulus (G'), loss modulus (G''), and the phase transition temperature (T_{pt}) of hydrogels. The corresponding values of ξ, WHC, hardness, G', and T_{pt} of produced hydrogels were found to be in the ranges of -23.3±1.52 to 6.3±0.25 mV; 4.6±0.22 to 98.9±0.16%; 0.4±0.15 to 14.3±0.81 N; 16,100 to 89,700 Pa; and 22 to 46 °C. Statistical analysis ($p<0.05$) showed that pH, solid content, and polymer ratio significantly influenced hydrogels' functional properties. However, as a general trend, the pH*solid content interaction was among the most critical factors influencing response variables.

Keywords: *Aloe vera*; rheological properties; hydrogels; blends; characterization.

Practical Application: This work studied the critical factors affecting the association of LAGG and AVG to generate experimental data and predictive equations for developing composite hydrogels for viscosity-texture adjustments of food products such as jams and jellies, fruit preparations, and dairy.

1 INTRODUCTION

Hydrogels are soft materials with solid and liquid properties consisting of a three-dimensional, cross-linked polymer network that can swell, absorb, and store a substantial amount of water (Ilgin et al., 2020; Martín-Illana et al., 2022). Hydrogels prepared from synthetic polymers are known as chemical hydrogels, while those made from natural polymers as physical hydrogels (Martín-Illana et al., 2022). Consequently, hydrogels' structure, strength, stability, and degradation time highly depend on the type of polymers and cross-links between the polymer chains. The covalent linkage is usually involved in chemical hydrogel preparation, whereas hydrophobic, electrostatic interactions, and hydrogen bonds are involved in physical hydrogels (Ilgin et al., 2020; Nele et al., 2020). Typically, fossil fuel industry products and cross-linking agents are used for chemical hydrogels, resulting in irreversible solid/semi-solid hydrogels with robust mechanical properties. Physical hydrogels, however, are preferred in medicine, food, and agriculture because biocompatible, degradable, nontoxic, low-cost, and renewable sources are used in their synthesis (Ahmad et al., 2023; Hajikarimi & Sadeghi, 2020).

This work studies the blend of natural polymers, namely gellan gum and *Aloe vera* gel (AVG), as alternatives for developing gelling matrices focused on food sciences' applications. Gellan gum is a linear anionic extracellular bacterial polysaccharide formed by a tetrasaccharide repeating unit consisting of two β-glucose, one β-glucuronic acid, and one α-rhamnose residue, commercially available in the form of high acyl (HAGG) and low acyl (LAGG) (Gomes et al., 2023). The molecular weight (MW) of HAGG in its native form ranges between 1 and 4 MDa, and, as a result of alkali diacylation, LAGG has an MW in the range of 200 to 300 kDa (Graham et al., 2019). The use of gellan gum in biomedicine, tissue engineering, and as a food additive has increased due to its versatile properties, low cost, and easy production at an industrial level (Gomes et al., 2023). However, for gelling purposes, it has been found that LAGG forms hard, non-elastic, brittle gels with T_{pt} from 30 to 50 °C, whereas HAGG gels are soft, elastic, and non-brittle with higher T_{pt} from 70 to 80 °C (Graham et al., 2019). Hydrogels with a broad range of textural and functional properties have been manufactured by blending the two gellan gum forms or in combination with different synthetic and natural polymers (Oliveira et al., 2021; Zhang et al., 2020a). From the literature review, however, mixtures of LAGG and AVG have been mainly

Received: 27 Jan., 2023
Accepted: 2 May, 2023
[1]*University of San Luis Potosi, Faculty of Chemical Science, San Luis Potosí, Mexico.*
[2]*Technological Institute of Tuxtla Gutiérrez, National Institute of Technology of Mexico, Tuxtla Gutiérrez, Mexico.*
*Corresponding author: mruiz@uaslp.mx

adopted to form edible films and coatings, with very few or no studies for manufacturing hydrogels (Ordoñez et al., 2021).

AVG refers to the transparent, viscous mucilage stored within the parenchyma cells in the leaves of Aloe plants. The gel is mainly composed of 98–99% water, and the rest is composed of compounds like polysaccharides, vitamins, minerals, enzymes, phenolic compounds, and organic acids (Maan et al., 2021). The content and type of solids can vary with the cultivars, harvesting, and season, where acetylated molecules of glucomannan (acemannan) are the primary polysaccharides, providing the gelling, biological, and medical properties of the raw gel (Maan et al., 2021). The acemannan has an MW of 1,000–1,600 kDa and is chemically composed of mannose, glucose, and galactose monomers (Liu et al., 2019). Due to its content of bioactive molecules, AVG is utilized in functional foods as a preservative and flavoring component in several drinks (Ahmad et al., 2023; Sempere-Ferre et al., 2022). However, due to the low mechanical properties of pure AGV, its primary use is mainly in the cosmetology and pharmaceutical industries (Martínez-Burgos et al., 2022). To create or improve its viscoelastic and rheological properties, hydrogels from AGV in combination with different polymers, such as cellulose, alginate, and pectin have been proposed in the literature (Patruni & Rao, 2023; Saad et al., 2021). Because biomacromolecule association/segregation in blends depends on factors such as ratios and polymer types, pH, temperature, and solid concentration, some investigations have also focused on controlling these factors (Patruni & Rao, 2023; Saad et al., 2021; Zhang et al., 2019). However, studies about using LAGG and AVG as an alternative for manufacturing hydrogels with potential applications in the food industry have yet to be explored. Therefore, this work aimed to study the association of LAGG and AVG for composite hydrogel creation and investigate the influence of pH, the solid content, and the polymer ratios.

2 MATERIALS AND METHODS

2.1 Raw materials

Analytical-grade LAGG powder (Phytagel™ product No. 71010-52-1; MW 1,000 g mol^{-1}; Gel strength ≥800 g cm^{-2}; pH 7; Sigma-Aldrich, St. Louis, MO, USA) without further treatment was used.

To obtain the AVG, the leaves with uniform maturity, size, color, and freshness of *Aloe Vera Barbadensis* Miller of approximately 2 years collected by an expert farmer in April 2021 in a plantation of the municipality of Río Verde, San Luis Potosí, Mexico, were used. Gel extraction was performed according to Maan et al. (2021) and Sempere-Ferre et al. (2022) with slight modifications. Adequately washed leaves with the respective average length and weight of 61.77±5.52 cm and 0.52±0.12 kg was selected and left immersed in distilled water in a vertical position for 48 h to promote the migration and removal of the yellow sap (aloin) contained in the middle layer of the leaves (Maan et al., 2021). Afterward, the fillets of gels were separated from the leaves with a spatula, subjected to several washes with distilled water, homogenized in a blender (IKA, Model T25 DS1, Staufen, Germany) at 2,000 rpm for 1 min, and frozen at -80 °C for 24 h. Samples were later freeze-dried (IlShinBioBase® Model TFD8501, Gyeonggi-do, South Korea) at -65 °C, with a vacuum of 5 mTorr for at least 90 h. Freeze-dried samples were ground with mortar and pestle into a fine powder, mixed, and then equilibrated in a desiccator over Drierite® (water activity≈0) at room temperature for several weeks to obtain a homogenous lot of fully dehydrated *Aloe vera* powder.

2.2 Physicochemical characterization of raw materials

A representative portion of the *Aloe vera* powder was used for its chemical composition assessment. The total content of polysaccharides was determined spectrophotometrically using phenol-sulphuric acid method (Zhang et al., 2020b). Briefly, 5 mL of 5% phenol solution was added to the 1 mL of 0.01% (w/v) of powder solution, followed by 5 mL of concentrated H_2SO_4. The absorbance at 490 nm was measured using a spectrophotometer (Thermo Fisher Scientific, Model Evolution 201, Madison, USA). The moisture content was determined gravimetrically by drying about 5 g of the powder in a vacuum oven at 70 °C under a pressure of 25 in Hg for 12 h (AOAC No. 934.06, AOAC, 2012). The ash content of 5 g of powder was estimated by incineration in a muffle furnace at 550 °C for 36 h (AOAC No. 923.03, AOAC, 2012). The Kjeldahl method involving digestion of 5 g of powder in 15 mL of concentrated sulfuric acid at 450 °C and titration with 0.1 N HCl was used to estimate the protein content (AOAC No. 960.52, AOAC, 2012). The lipid content of 5 g of powder was determined using the Soxhlet method extraction with 250 mL of hexane at 80 °C for 6 h, followed by the total removal of the solvent by evaporation (AOAC No. 960.39, AOAC, 2012). Measurements were made in triplicate.

Fourier transform infrared spectroscopy (FTIR), and zeta potential (ξ) with hydrogels of pure polymers were implemented to characterize the chemical structure and surface charges of both components. LAGG and AVG solutions were prepared with a solid content of 0.50 (w/v) at the natural pH dispersing under magnetic stirring for 20 min at 90°C for solutions containing LAGG and 10 min at 50 °C for AVG ones. A Nicolet spectrometer with an attenuated total reflectance detector (Thermo Fisher, Model iZ10, Madison, USA) operating in the range of 4,000–400 cm^{-1} and with a spectral resolution of 4 cm^{-1} was used. An average of 40 scans was performed for each sample at room temperature. The ξ values of the LAGG and AVG solutions were determined using Zetasizer Nano equipment (Malvern Instruments, Model ZS90, Worcestershire, UK) in the pH range of 1 and 9.3. Samples were poured into the DTS1060 capillary cell for measurement at room temperature. All measurements were in triplicate.

2.3 Synthesis of LAGG/AVG hydrogels

A face-centered central composite design with five center points was employed to evaluate the effect of pH (1, 4, and 7), polymer ratio (66:33, 50:50, and 33:66 LAGG/AVG), and solid content (0.25, 0.50, and 0.75 w/v) on the physicochemical, textural, and rheological properties of the produced hydrogels. A total of 19 different hydrogels were created, as shown in Table 1.

Table 1. Experimental design and measured response variables for the binary composite hydrogels of low acyl gellan gum (LAGG) and *Aloe vera* gel (AVG).

Exp		Factors			Response variables							
No	**Ro**	***A*** **pH**	***B*** **LAGG/AVG**	***C*** **w/v**	**ξ mV**	**WHC %**	**Hardness N**	n'	k' $Pa.s^{n'}$	n''	k'' $Pa.s^{n'}$	T_{pt} **range (°C)**
8	1	7	66/33	0.75	6.3±0.25	97.7±0.14	6.9±1.02	0.061	48,743.8	-0.017	6,916.2	37–46
6	2	7	33/66	0.75	-2.3±1.62	98.9±0.16	8.4±0.23	0.064	38,613.5	-0.010	5,357.3	36–42
12	3	4	66/33	0.5	-3.2±5.23	78.1±5.45	13.1±0.23	0.085	48,052.4	-0.111	10,089.1	23–40
10	4	7	50/50	0.5	-3.8±4.46	97.1±0.43	5.2±0.72	0.055	36,399.7	-0.034	4,859.1	31–40
5	5	1	33/66	0.75	-2.6±1.30	95.8±1.16	7.4±0.66	0.069	48,231.4	-0.088	8,212.0	32–41
3	6	1	66/33	0.25	-6.6±1.33	98.1±1.66	1.5±0.61	0.047	24,915.5	-0.063	2,982.3	25–36
14	7	4	50/50	0.75	-3.4±11.44	98.4±0.09	10.3±0.35	0.079	44,430.2	-0.082	7,497.4	37–44
19	8	4	50/50	0.5	-9.5±2.24	97.6±0.18	6.1±0.96	0.054	28,072.2	-0.021	3,625.1	25–29
11	9	4	33/66	0.5	-9.3±2.27	95.3±1.05	3.4±0.20	0.078	42,314.8	-0.112	7,608.9	25–35
15	10	4	50/50	0.5	-7.9±8.40	96.1±0.33	7.0±0.32	0.056	28,682.8	-0.051	3,742.7	24–32
17	11	4	50/50	0.5	-13.3± 3.31	96.1±0.35	6.0±0.29	0.045	27,195.8	-0.024	2,718.7	25–33
16	12	4	50/50	0.5	-14.5±4.42	96.2±0.61	4.6±0.16	0.060	28,954.1	-0.008	3,778.6	25–32
2	13	7	33/66	0.25	-11.8±0.75	4.6±0.22	0.4±0.15	0.059	20,330.1	-0.130	3,076.5	25–35
1	14	1	33/66	0.25	-9.5±3.20	89.9±3.15	0.6±0.38	0.054	22,190.3	-0.073	2,946.4	27–35
13	15	4	50/50	0.25	-17.6± 2.17	79.4±2.63	0.8±0.34	0.046	27,995.3	-0.103	3,499.2	28–38
9	16	1	50/50	0.5	-4.0±1.72	89.5±2.01	10.3±0.38	0.058	42,960.8	-0.160	7,179.4	22–32
4	17	7	66/33	0.25	-23.3±1.52	14.8±1.97	N.D.	0.060	19,547.7	-0.050	2,984.7	28–35
18	18	4	50/50	0.5	-12.9±0.36	97.0±0.38	6.6±0.28	0.056	27,049.2	-0.008	3,853.5	25–32
7	19	1	66/33	0.75	-21.3±1.40	97.8±0.26	14.3±0.81	0.087	59,831.8	-0.046	7,693.2	32–41

Ro: run order; N.D.: not determined; *A*: pH; *B*: polymer ratio; *C*: solid content; ξ: zeta potential; WHC: water holding capacity; k' and k'': the intercepts; n' and n'': the slopes of G' and G'' frequency dependence, respectively; T_{pt}: phase transition temperature.

Due to high hydration temperature of LAGG, starting solutions based on this gum were used in synthesizing hydrogels. The required amount of LAGG was dispersed in distilled water at 90 °C in a water bath, followed by magnetic stirring for about 20 min for complete hydration. The solutions were contained in airtight containers to prevent moisture loss by evaporation. The solution was then cooled to 60 °C, adjusting the pH with NaOH and HCl solutions (0.1 M). Then, the required amount of AVG was added and dispersed with magnetic stirring for about 10 min to obtain a clear or transparent solution. Preliminary tests determined the setting temperature of 60 °C to achieve mixtures without previous gelling of the gum. The solid content of the solutions was verified with a digital refractometer (Leica AR 200) at 60 °C adjusting it by adding distilled water in case of moisture loss. The solutions were cooled in cold water baths at 8–10 °C for 20 min. The synthesized hydrogels were stored at 4 °C in a refrigerator for 24 h to ensure complete gelation.

2.4 Physicochemical characterization of hydrogels

The ξ values of the hydrogels were determined using the same equipment and procedure as indicated in Section 2.2. LAGG/AVG solutions at 60 °C were transferred to the DTS1060 capillary cell and equilibrated at room temperature for their corresponding measurement. The procedure of Alavi et al. (2020) was used for water holding capacity (WHC) measurements. The synthesized hydrogels in 5 mL tubes were centrifuged at 8,000 g for 10 min at 8 °C using a refrigerated centrifuge (Sigma, model 3-18K, Osterode am Harz, Germany). The water released by the samples was carefully withdrawn with a syringe and then weighed. The WHC was calculated using Equation 1:

$$\text{WHC (\%)} = \frac{w_i - w_o}{w_i} \times 100 \quad (1)$$

Where:

wi: the mass of water in gels before centrifugation;

wo: the mass of released water.

The ξ and WHC measurements were made in triplicate for each sample.

2.5 Hardness characterization of hydrogels

The compressive toughness testing of hydrogel was applied to measure its hardness (Ozel & Oztop, 2023). Cylindrical hydrogels with a diameter of 25 mm and a height of about 30 mm were synthesized in beakers and stored at 4 °C for 24 h before analysis. The formed gels were carefully separated from the beakers with the help of a spatula (Heathrow Scientific HD15907) and then removed by gravity from the inverted containers. The gels were then equilibrated at room temperature for 30 min and then compressed up to 80% strain using a speed of 5 mm s^{-1} with a Stable Micro Systems Texture Analyser (Texture Technologies, Model TA-XT plus, Godalming, UK). The maximum required force to rupture the gel was defined as gel hardness. Measurements were made in triplicate for each sample.

2.6 Rheological characterization of hydrogels

The rheological properties of hydrogels were characterized by a rotational rheometer (Anton Paar Physica, Model MCR

302, Graz, Austria) equipped with a conical stainless-steel plate (with a 49.977-mm diameter, a 1.992° cone angle, and a 1-mm gap) and a Peltier system (H-PTD 200) for temperature control. Start Rheoplus US 200 software was used to set experimental conditions and analyze data. About 1.5 mL of LAGG/AVG samples at 60 °C were transferred onto the rheometer plate. The samples were carefully covered with low-viscosity mineral oil to minimize moisture loss during measurement. Frequency sweep tests were performed at 5 °C in the range of 0.1–100 rad s^{-1} within the linear viscoelastic region (LVR) using a strain amplitude of 0.05% (Alghooneh et al., 2019). Hydrogels' elastic and viscous characteristics were analyzed through recorded G' and G'' as a function of angular frequency (ω). Cooling sweep tests were performed from 80 to 5 °C at 1 °C min^{-1}, according to Oliveira et al. (2020), with slight modifications to evaluate the gelation behavior. For this purpose, a frequency between 0.2 and 0.5 Hz and strain values of 1–0.1% from 80 to 25 °C and 0.05% from 25 to 5 °C within the LVR were used. The G', G'', phase angle (δ), and complex viscosity (n^*) profiles versus temperature were analyzed to monitor the T_{pt} of produced hydrogels (Oliveira et al., 2020).

2.7 Statistical analysis

A second-order polynomial equation (Equation 2) was used to evaluate the effect of pH (A), polymer ratio (B), and solid content (C) on the response variables (ξ, WHC, hardness, k', n', k'' and n'') given in Table 1.

$$y = \beta_0 + \beta_1 A + \beta_2 B + \beta_3 C + \beta_4 AB + \beta_5 AC + \beta_6 BC + \beta_7 A^2 + \beta_8 B^2 + \beta_9 C^2 + \beta_{10} ABC + \beta_{11} A^2 B + \beta_{12} A^2 C + \beta_{13} AB^2 \quad (2)$$

Where:

β_0 to β_{13}: the regression coefficients of the model.

The analysis was carried out with a confidence level of 95% ($p<0.05$) using the MODDE 7.0 software (Umetrics, Kinnelon, NJ, USA). A Box-Cox transformation for stabilizing the prediction variance was performed in some cases. Only hierarchical equations were considered using the backward pruning technique with an α out of 0.10.

3 RESULTS AND DISCUSSION

3.1 Polymers characterization

The *Aloe vera* powder was found to be composed of approximately 4.12±0.07% water, 10.23±0.78% lipids, 7.87±1.56% protein, 29.13±1.57% ash, and 48.45±1.18% carbohydrates, which agree with those reported in the literature (Martínez-Burgos et al., 2022; Patruni & Rao, 2023). In *Aloe vera* powder, carbohydrates are the significant components, followed by minerals and proteins. Therefore, AGV can also be considered an important source of proteins and essential micronutrients such as K, Ca, Cl, and Mg.

The FTIR spectra showing the main functional groups of the pure LAGG and AVG hydrogels measured at room temperature are presented in Figure 1A. This figure illustrates that both hydrogels exhibit at least four similar peaks but with more intense bands for the AVG gel. For instance, the characteristic peak of hydrogen bonds corresponding to the -OH groups was observed at 3,282 cm^{-1} in LAGG and 3,276 cm^{-1} in AVG. The LAGG exhibits stretching vibrations of the C-H groups at 2,879 cm^{-1} and the AVG at 2,893 cm^{-1}.

The presence of glycosidic bonds and hydroxyl groups was detected at 1,601 and 1,022 cm^{-1} in LAGG and 1,590 and 1,021 cm^{-1} in AVG (Kazemi-Taskooh & Varidi, 2021). The additional bands observed at 1,730 and 1,238 cm^{-1} in AVG hydrogel are attributed to C=O and C–O– stretches of acetyl groups resulting from the polysaccharide acemannan, which play an essential role in the interaction of acemannan with other biomolecules (Alvarado-Morales et al., 2019; Patruni & Rao, 2023). However, due to significant amount of minerals in the powder and since the gel's strength increases with increasing ion concentration, it can also be assumed that minerals promote the interaction of mixture of AVG with other molecules.

The surface electrical properties of the pure LAGG and AVG hydrogels characterized by the ξ values as a function of the pH are shown in Figure 1B. Both polymers showed negatively charged components throughout the entire pH range studied, where the ξ values for LAGG were significantly higher than those for AVG. The ξ is also a parameter used to predict the stability of food systems since the higher this value, the more stable the system is (Serrano-Lotina et al., 2022). Figure 1B shows that the ξ for the LAGG hydrogel continuously decreased from -0.96 to -16.2 mV between pH 1 and 5 and remained almost constant up to the pH of 9. The anionic character as a function of the pH of gellan gum with a pKa of 3 has been reported in the literature (Duarte et al., 2022). Regarding the ξ of AVG hydrogel, this decreased from -11.9 to -30 mV between pH 1 and 4 and remained almost constant up to the pH of 9. Complete ionization of the hydroxyl groups in polymers has been related to the nonvariation of ξ with pH (Zhang et al., 2019).

3.2 Physicochemical and textural properties of hydrogels

The correlation between pH, polymer ratio, and solid content as independent factors on response variables given in Table 1 was performed using response surface analysis. The coded regression coefficients, the determination coefficient (R^2), the adjusted R^2, and the coefficients of variation (CV%) obtained with Equation 2 for each of the dependent variables are in Table 2. The highlighted regression coefficient in the model shows that the effect on the response is statistically significant ($p<0.05$). The models interpreted data variability with R^2, adj R^2, and CV between 0.717 and 0.999, 0.576 and 0.997, and 0.78 and 47.7%, respectively, indicating good acceptability of fitted models.

The ξ values measured in the synthesized hydrogels ranged from -23.3±1.52 to 6.3±0.25 mV, in which Experiment 4 showed the lowest value and Experiment 8 the highest (Table 1).

As previously mentioned, the higher the ξ value, the more stable the system is. Values of this order of magnitude can result

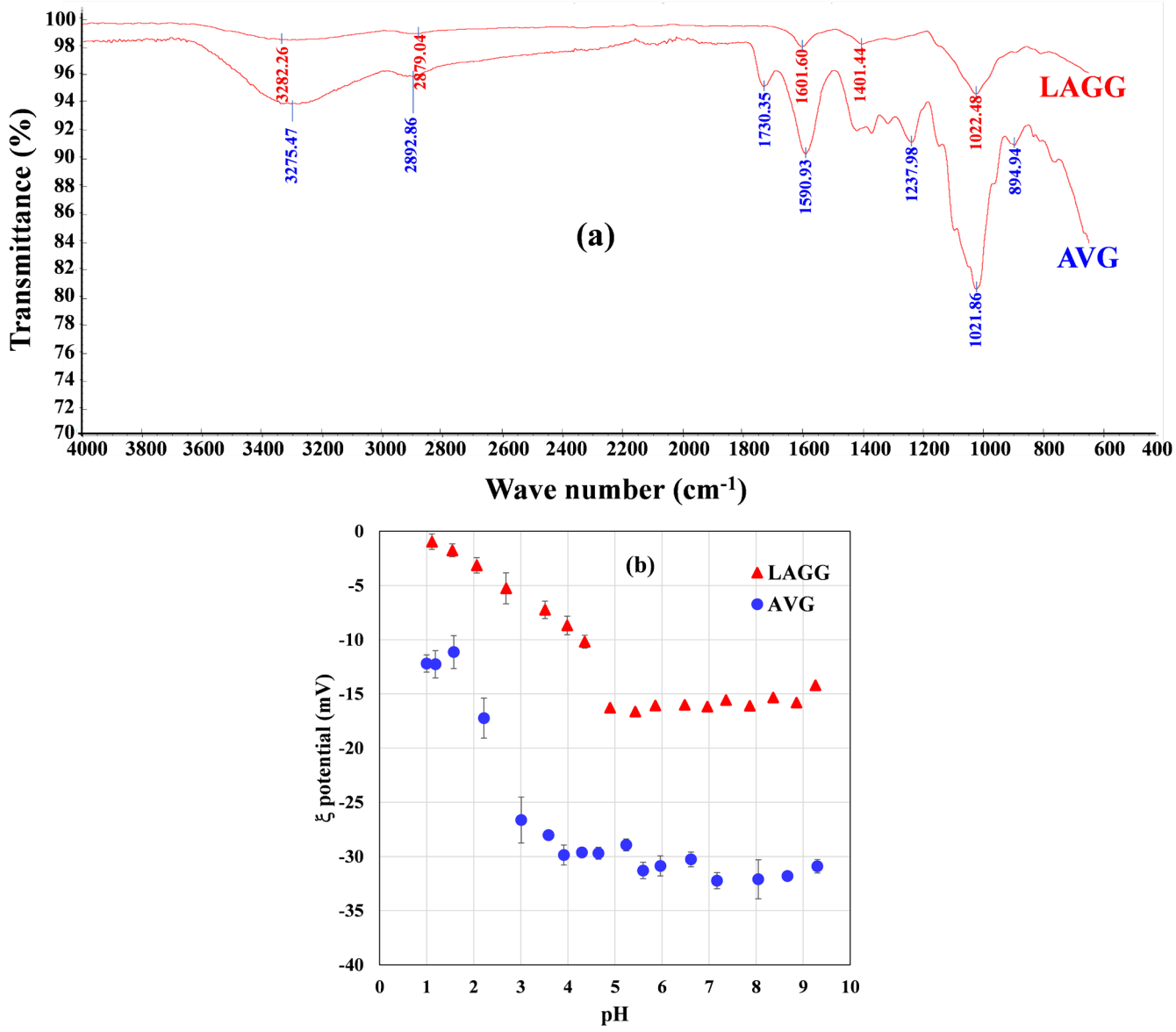

Figure 1. FTIR spectrum at (A) natural pH and (B) ξ potential as a function of pH measured in pure LAGG and AVG hydrogels at fixed solid content of 0.5 w/v.

in good or acceptable short-term stability for the food systems (Serrano-Lotina et al., 2022). Figure 2A shows the variation of ξ as a function of pH and solid content. According to Table 2, ξ was mainly affected by the pH*solid content interaction followed by the pH*polymer ratio*solid content interaction and, to a lesser degree, by the solid content. Among the functional properties of hydrogels, WHC is one of the most important, defined as the gel's water content in equilibrium with its serum phase (Alavi et al., 2020). Therefore, hydrogels in nonequilibrium and metastable states can expel water and show syneresis. The latter means that syneresis decreases as the WHC increases or vice versa. Thus, the ability of hydrogels to retain water or active substances within the network is usually associated with WHC values (Alavi et al., 2020). Temperature, polymer concentration, pH, and conditions used to induce gelation are among the most critical factors affecting the cross-linking of the polymers and, consequently, the WHC and stability of the hydrogel (Ilgin et al., 2020).

From Table 1, WHC and hardness values of prepared gels ranged respectively, from 4.6±0.22 to 98.9±0.16% and from 0.4±0.15 to 14.3±0.81 N. Figures 2B and 2C represent the response surface plots for the effect of pH and solid content on WHC and hardness at a fixed polymer ratio of 50:50. Generally, gels with a pH below 4 and solid content of 0.75 w/v showed the highest values of WHC and the lowest with 0.25 w/v and a pH above 4 (Figure 2B). Except for the pH*polymer ratio interaction, all the model terms (Equation 2) significantly affected WHC. It is also noted that pH*solid content interaction was among the most critical factors influencing WHC. Texture analyses evaluate the extent of failure and durability of soft materials such as hydrogels (Ozel & Oztop, 2023). Therefore, the hardness is also given in Table 1. Visually, hardness represents the gel's firmness and, structurally, measures the force required to

Table 2. Regression coefficients (coded variables) of Equation 2 and statistical parameter values for different responses of Table 1 ($p<0.05$).

γ	β_0	β_1	β_2	β_3	β_4	β_5	β_6	β_7	β_8	β_9	β_{10}	β_{11}	β_{12}	β_{13}	R^2	Adj R^2	CV (%)
ξ	-8.97	0.91	-1.26	4.55	1.61	5.86	-0.19	-	-	-	5.21	-	-	-	0.787	0.651	47.69
P>F	**0.0052**	0.5152	0.3718	**0.0063**	0.3094	**0.0026**	0.9036				**0.0055**						
WHC	96.7	3.80	-8.60	9.50	-0.15	21.45	-2.20	-3.67	-10.27	-8.07	-0.65	11.0	13.35	-24.50	0.999	0.997	0.78
P>F	**<1E-03**	**5E-04**	**<1E-03**	**<1E-03**	0.553	**<1E-03**	**2E-03**	**3E-03**	**<1E-03**	**< E-03**	**0.0402**	**<1E-03**	**<1E-03**	**< E-03**			
Hardness	5.99	-2.55	5.12	4.75	3.24	-5.04	-3.84	1.48	1.98		-5.34	-4.89	-	5.99	0.985	0.957	13.42
P>F	**1E-03**	**0.0052**	**<1E-03**	**2E-03**	**0.0020**	**2E-03**	**8E-03**	**0.0353**	**0.0111**		**1E-03**	**0.0013**		**4E-03**			
n′	0.059	-2.4E-03	2.5E-03	0.010	-	-7.2E-03	-	-9.1E-03	0.016	-	-	-	-	-	0.717	0.576	14.13
P>F	**0.0082**	0.397	0.393	**0.003**		**0.0383**		**0.0497**	**0.0076**								
k′	27,991	-3281	2,868.8	8,217.4	-30,417	-31,479	32,268	11,690	17,193	8,221.9	-29,540	29,885	35,132	-30,006	0.998	0.993	2.55
P>F	**< 1E-03**	**0.0056**	**0.0090**	**2E-04**	**<1E-03**	**<1E-03**	**<1E-03**	**<1E-03**	**<1E-03**	**3E-04**	**<1E-03**	**<1E-03**	**<1E-03**	**<1E-03**			
n′′	-0.022	0.063	3.7E-04	0.011	0.20	0.22	-0.20	-0.075	-0.089	-0.070	0.18	-0.18	-0.19	0.14	0.965	0.852	28.06
P>F	**0.0258**	**0.0075**	0.978	0.443	**0.0022**	**0.0016**	**0.0020**	**0.0075**	**0.0040**	**0.0093**	**0.0031**	**0.0043**	**0.0038**	**0.0104**			
k′′	3,543.7	-1160.1	1,240.1	1,999.1	-8,014.3	-8,728.5	8,395.0	2,475.5	5,305.3	1,954.6	-7,982.4	7,140.9	8,282.5	-7,535.3	0.990	0.957	9.27
P>F	**0.0024**	**0.0249**	**0.0201**	**0.0038**	**4E-04**	**3E-04**	**4E-04**	0.0032	**2E-04**	**0.0076**	**4E-04**	**9E-04**	**5E-04**	**8E-04**			

P>F: Fisher probability; CV coefficient of variation; ξ: zeta potential; WHC: water holding capacity; *k′* and *k′′*: the intercepts; *n′* and *n′′*: the slopes of *G′* and *G′′* frequency dependence, respectively. Bold values indicate that the corresponding parameter significantly affected the properties evaluated.

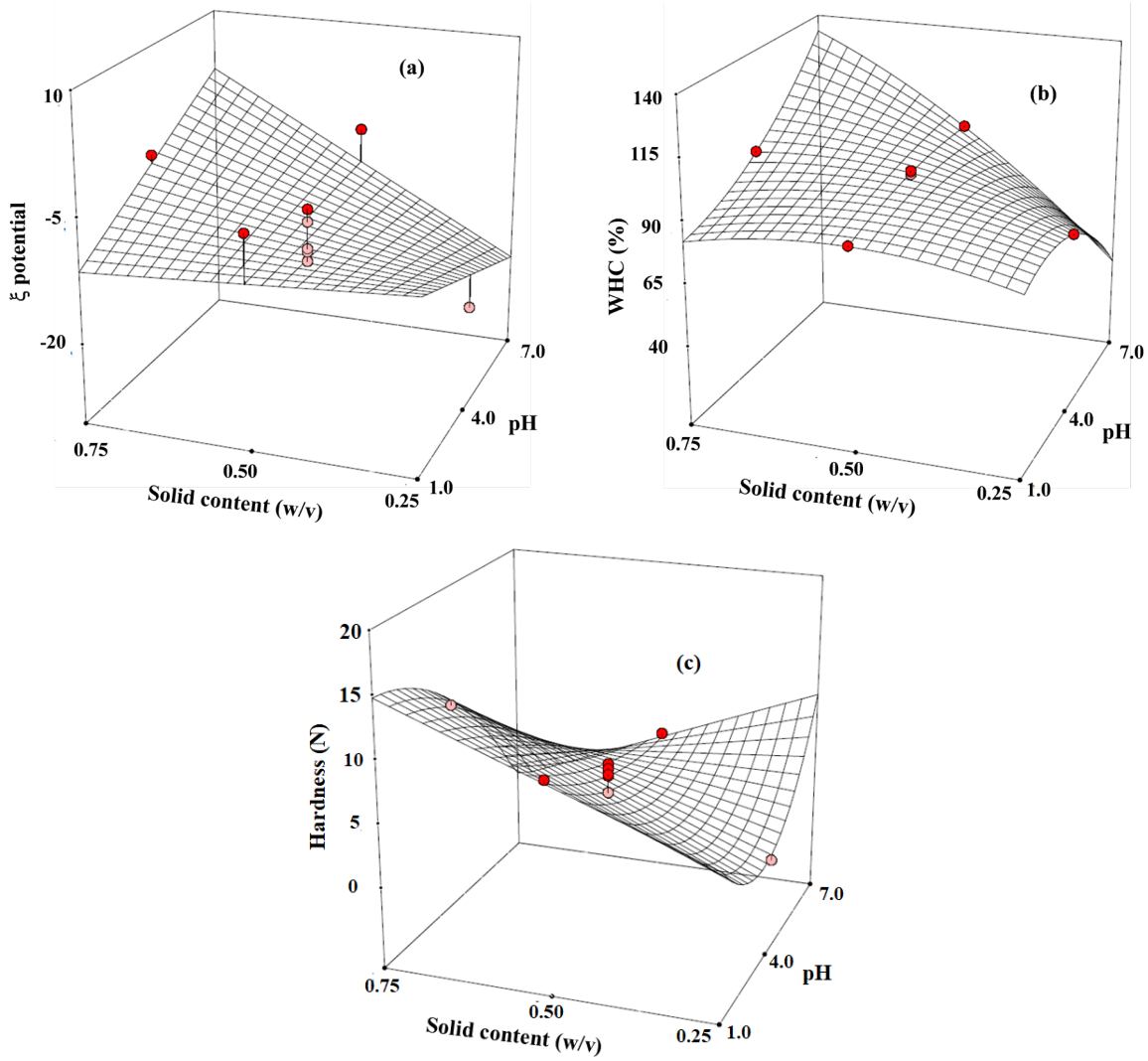

• Experimental data.

Figure 2. Response surface plots showing the effect of (A) the solid content and pH on ξ potential, (B) WCR, and (C) hardness of hydrogels at fixed polymer ratio of 50:50.

break the gel (Mousavi et al., 2019). Figure 2C shows an increase in hardness values with an increase in solid content and a decrease in pH for a fixed polymer ratio of 50:50. According to Table 2, effects of pH, polymer ratio, and solid content with their linear interactions and quadratic terms were observed for hardness values.

3.3 Rheological properties of hydrogels

To help understand the viscoelastic properties of LAGG/AVG hydrogels, the values of G' and G'' as a function of ω were measured, as shown in Figure 3. The facility of a material to store energy elastically is represented by G', while G'' indicates the energy dissipation when the same material is subjected to oscillatory deformation (Rahmatpour et al., 2023). Thus, the higher the value of G', the more difficult it is to decompose the polymer. Figure 3 shows that all the hydrogels exhibited mechanical spectra with G' and G'', showing discrete frequency dependence. The G' values were consistently higher than G'' throughout the entire frequency range, indicating that hydrogel samples behaved as a typical gel-like material response (Alghooneh et al., 2019; Rahmatpour et al., 2023). This confirms that blends of LAGG/AVG are highly effective at low-use levels in forming gels. Likely, *Aloe vera*'s acetylated groups and high mineral content have contributed significantly to gel formation. Among the experimental conditions tested, Experiment 7, conducted with a pH of 1, 66:33 ratio, and 0.75 w/v (Table 1), showed the highest values of G', ranging from 49,500 to 89,700 Pa. Conversely, the gels of Experiments 2 and 4 made with a pH of 7, 0.25 w/v, and respective ratios of 33:66 and 66:33 (Table 1), presented the lowest values of G', varying from 16,900 to 26,100 Pa and from 16,100 to 25,800 Pa. Intermediate G' values ranging from 23,400 to 36,900 Pa were determined for the rest of the gels. Frequency sweep tests, such as those shown in Figure 3, have also been used to differentiate between solid and soft hydrogels from entangled solutions (Alghooneh et al., 2019; Rahmatpour et al., 2023).

As Alghooneh et al. (2019) and Patruni and Rao (2023) suggested, the frequency dependence of G' and G'' was evaluated using power law model parameters with Equations 3 and 4:

$$G' = k'\omega^{n'} \quad (3)$$

$$G'' = k''\omega^{n''} \quad (4)$$

Where:

k' ($Pa.s^{n'}$) and k'' ($Pa.s^{n''}$):the intercepts;

n' and n'': the slopes of G' and G'' frequency dependence, respectively.

The k', k'', n', and n'' values for each experimental condition are given in Table 1. The contribution of the viscous component to the elastic component was determined by the ratio between k'' and k'. According to the classification proposed by Alghooneh et al. (2019), the rheological properties of all LAGG/AVG hydrogels synthesized in this work correspond to semisoft gels as revealed by the following: $0.100 \leq {}^{k''}/_{k'} \leq 0.210$, $0.045 \leq n' \leq 0.087$, $-0.160 \leq n'' \leq -0.08$, and $8.5 \leq {}^{G''}/_{G'} \leq 11.7$. This final relation was determined at the maximum ω value.

Table 2 shows that the linear interaction and quadratic terms of the pH, polymer ratio, and solid content significantly affected both the k' and k'' values. On the contrary, n' and n'' were significantly affected by interaction and quadratic terms of pH, polymer ratio, and solid content. It is also noted that pH*solid content interaction was one of the most critical factors affecting k', k'', n', and n'', with the highest values generally at a pH of 1 and solid content of 0.75 w/v.

Figures 4A and 4B illustrate, for example, the change of G', G'', η*, and δ during the cooling sweep of the solutions of Experiments 7 and 4, respectively. Commonly, gels' sol-gel T_{pt} is determined when G' equals G'' during a cooling sweep test. A crossover of G' and G'' was not observed, because G' was consistently higher than G'' within the temperature range studied. On the contrary, the hydrogels exhibited rheograms with gradual increases initially, continuing with sharp rises of G' and G'' as the

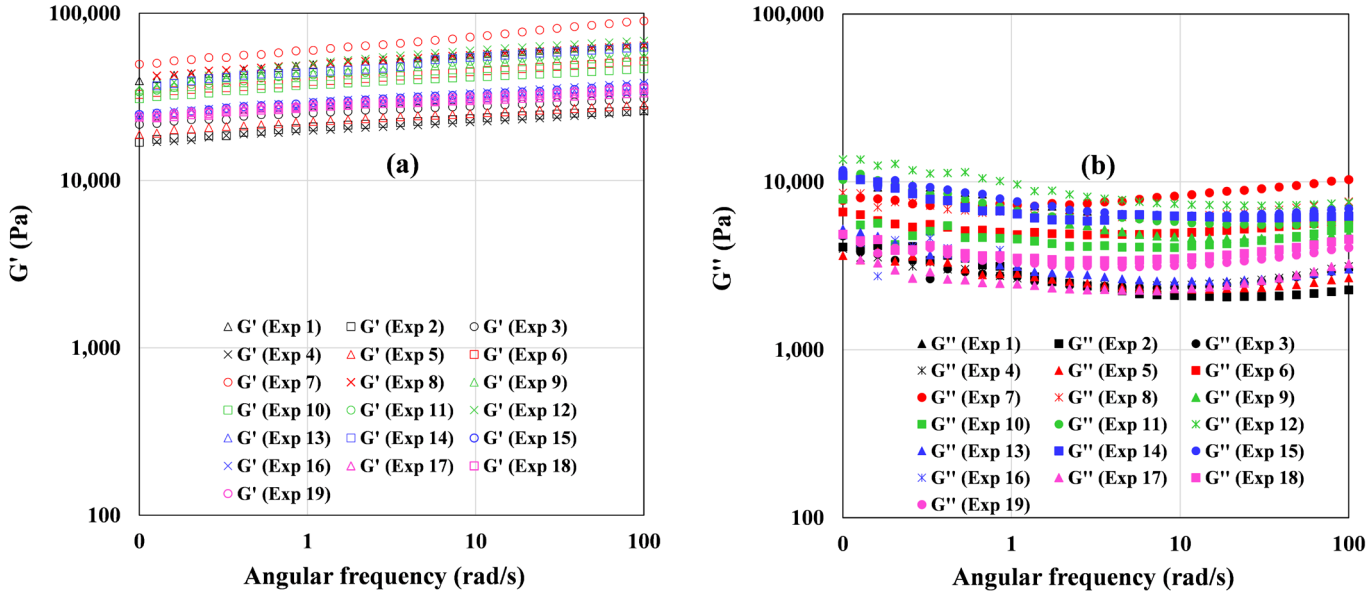

Figure 3. Variation of G' (a) and G' (b) with ω for the binary composite hydrogels of LAGG/AVG at 5°C and 0.05% strain.

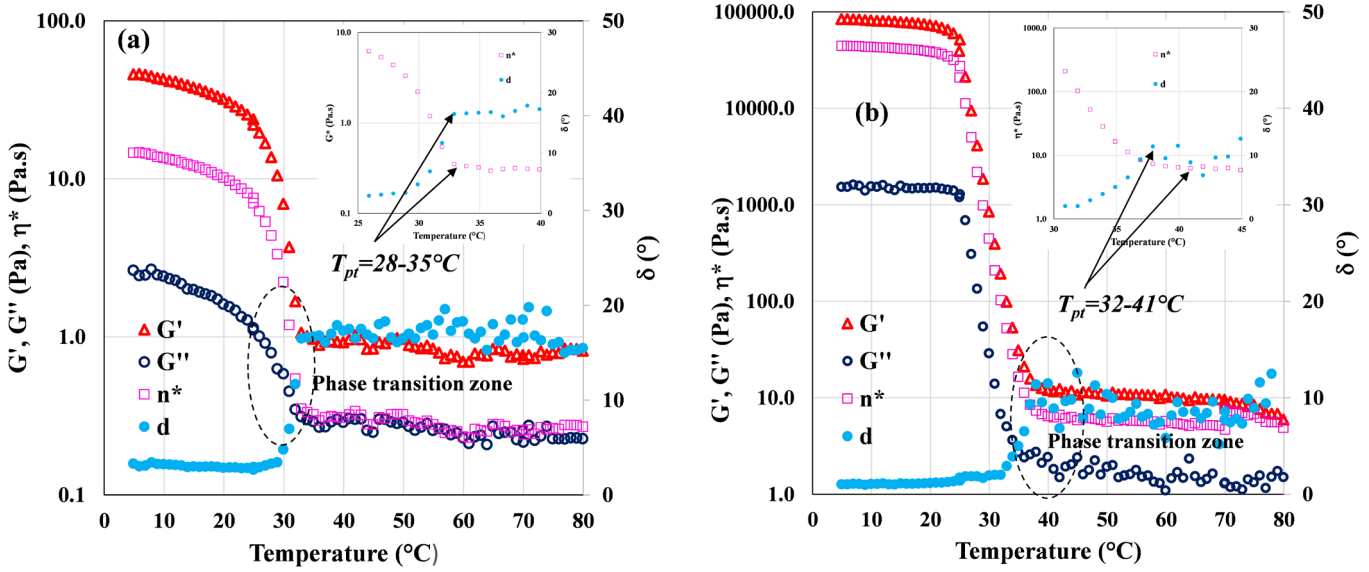

Figure 4. Temperature dependence of G', G'', η*, and δ during the cooling sweep of LAGG/AVG solutions of (A) Exp 4 and (B) Exp 7. The insert figure highlights the T_{pt} range of the hydrogels.

temperature decreased. Rheological behaviors with these trends suggest that the gelation process of natural polymers is more complex than synthetic polymers because of the involvement of factors such as coil-helix transitions, disulfide, and hydrogen bonds (Oliveira et al., 2020). Likely, the gelation process occurs over a temperature range; a single gelation point does not define the process. Figures 4A and 4B show that the temperature range at which G' and G'' rise strongly depends on the type of hydrogel. Thus, the temperatures at which η* and δ reached a plateau were used to estimate the T_{pt} range of the hydrogels as indicated in the inserted graphs in Figure 4 (Graham et al., 2019; Oliveira et al., 2020). The T_{pt} of the produced hydrogels ranged between 22 and 46 °C (Table 1), consistent with the reported gelation temperature for gellan gum and gellan gum-xanthan gels (Graham et al., 2019). Gel formation was also tested by the inverted tube method at 25 °C. All the hydrogels were translucent and transparent, and the only hydrogel that could not support its weight was the one synthesized in Experiment 4 at a pH of 7, 66:33 ratio, and 0.25 w/v.

Hydrogels with a T_{pt} above room temperature and close to physiological temperatures, as proposed herein, could be ideal candidates for gelling purposes in the food industry.

4 CONCLUSION

A series of 19 hydrogels were prepared by blending LAGG and AVG, varying the pH, polymer ratio, and solid content, and studying the structural, physicochemical, and rheological properties. The results showed that all the composite hydrogels exhibited G' larger than G'' throughout the tested frequency range, with mechanical parameters corresponding to elastic and semi-soft gels and T_{pt} ranging from 22 to 46 °C. The chemical characterization of *Aloe vera* powder showed that substantial amounts of minerals and proteins are present in addition to carbohydrates, contributing significantly to the gel formation. However, from the structural and physicochemical point of view, broad ranges of values of WHC (4.6±0.22 to 98.9±0.16%) and hardness (0.4±0.15 to 14.3±0.81 N) were obtained. This confirms that WHC, hardness, and rheological properties are complementary tests to discriminate the functional properties of hydrogels and their proper use. Statistical analysis ($p<0.05$) showed that the pH*solid content interaction was among the most critical factors influencing response variables. Predictive equations ($R^2>0.727$ and CV<47.7%) of ξ, WHC, hardness, k', n', k'', and n'' as a function of pH, polymer ratio, solid content, and their interactions are given in this study. However, further experiments are necessary to validate obtained equations.

Acknowledgments

The authors acknowledge the Mexican National Council of Science and Technology (CONACyT) with the project CB2017-2018/A1-S-32348 and the scholarship provided to Verónica Guadalupe Hernández-Briones for her PhD study. The laboratory assistance of Mrs. C. Rivera-Bautista is gratefully acknowledged.

References

Ahmad, M., Ali, S. W., Hameed, A., Amir, M., Ashrad, J., Afzal, M. I., Umer M., Alsagaby, S. A., Awais, M., Imran, M., Iqbal, S., Ahmed, A., & Riaz, M. (2023). Functional potential of *Aloe vera* juice against CCl_4 induced hepatotoxicity in animal model. *Food Science and Technology*, 43, e110321. https://doi.org/10.1590/fst.110321

Alavi, F., Emam-Djomeh, Z., Momen, S., Hosseini, E., & Moosavi-Movahedi, A. A. (2020). Fabrication and characterization of acid-induced gels from thermally-aggregated egg white protein formed at alkaline condition. *Food Hydrocolloids*, 99, 105337. https://doi.org/10.1016/j.foodhyd.2019.105337

Alghooneh, A., Razavi, S. M. A., & Kasapis, S. (2019). Classification of hydrocolloids based on small amplitude oscillatory shear, large amplitude oscillatory shear, and textural properties. *Journal of Texture Studies*, *50*(6), 520-538. https://doi.org/10.1111/jtxs.12459

Alvarado-Morales, G., Minjares-Fuentes, R., Contreras-Esquivel, J. C., Montañez, J., Meza-Velázquez, J. A., & Femenia, A. (2019). Application of thermosonication for *Aloe vera* (*Aloe barbadensis Miller*) juice processing: Impact on the functional properties and the main bioactive polysaccharides. *Ultrasonics Sonochemistry*, *56*, 125-133. https://doi.org/10.1016/j.ultsonch.2019.03.030

Association of Official Analytical Chemists (AOAC) (2012). *Official methods of analysis of the Association of Official Analytical Chemistry*. Association of Official Analytical Chemists.

Duarte, L. G. R., Alencar, W. M. P., Iacuzio, R., Silva, N. C. C., & Picone, C. S. F. (2022). Synthesis, characterization and application of antibacterial lactoferrin nanoparticles. *Current Research in Food Science*, *5*, 642-652. https://doi.org/10.1016/j.crfs.2022.03.009

Gomes, D., Batista-Silva, J. P., Sousa, A., & Passarinha, L. A. (2023). Progress and opportunities in Gellan gum-based materials: A review of preparation, characterization and emerging applications. *Carbohydrate Polymers*, *311*, 120782. https://doi.org/10.1016/j.carbpol.2023.120782

Graham, S., Marina, P. F., & Blencowe, A. (2019). Thermoresponsive polysaccharides and their thermoreversible physical hydrogel networks. *Carbohydrate Polymers*, *207*, 143-159. https://doi.org/10.1016/j.carbpol.2018.11.053

Hajikarimi, A., & Sadeghi, M. (2020). Free radical synthesis of cross-linking gelatin base poly NVP/acrylic acid hydrogel and nanoclay hydrogel as cephalexin drug deliver. *Journal of Polymer Research*, *27*, 57. https://doi.org/10.1007/s10965-020-2020-1

Ilgin, P., Ozay, H., & Ozay, O. (2020). Synthesis and characterization of pH responsive alginate based-hydrogels as oral drug delivery carrier. *Journal of Polymer Research*, *27*(9), 251. https://doi.org/10.1007/s10965-020-02231-0

Kazemi-Taskooh, Z., & Varidi, M. (2021). Designation and characterization of cold-set whey protein-gellan gum hydrogel for iron entrapment. *Food Hydrocolloids*, *111*, 106205. https://doi.org/10.1016/j.foodhyd.2020.106205

Liu, C., Cui, Y., Pi, F., Cheng, Y., Guo, Y., & Qian, H. (2019). Extraction, purification, structural characteristics, biological activities and pharmacological applications of acemannan, a polysaccharide from *Aloe vera*: A review. *Molecules*, *24*(8), 1554. https://doi.org/10.3390/molecules24081554

Maan, A. A., Ahmed, Z. F. R., Khan, M. K. I., Riaz, A., & Nazir, A. (2021). *Aloe vera* gel, an excellent base material for edible films and coatings. *Trends in Food Science & Technology*, *116*, 329-341. https://doi.org/10.1016/j.tifs.2021.07.035

Martínez-Burgos, W. J., Lima Serra, J., Marsiglia F, R. M., Montoya, P., Sarmiento-Vásquez, Z., Marin, O., Gallego-Cartagena, E., & Paternina-Arboleda, C. D. (2022). *Aloe vera*: From ancient knowledge to the patent and innovation landscape- A review. *South African Journal of Botany*, *147*, 993-1006. https://doi.org/10.1016/j.sajb.2022.02.034

Martín-Illana, A., Notario-Pérez, F., Cazorla-Luna, R., Ruiz-Caro, R., Bonferoni, M., Tamayo, A., & Veiga, M. (2022). Bigels as drug delivery systems: From their components to their applications. *Drug Discovery Today*, *27*(4), 1008-1026. https://doi.org/10.1016/j.drudis.2021.12.011

Mousavi, S. M. R., Rafe, A., & Yeganehzad, S. (2019). Textural, mechanical, and microstructural properties of restructured pimiento alginate-guar gels. *Journal of Texture Studies*, *50*(2), 155-164. https://doi.org/10.1111/jtxs.12385

Nele, V., Wojciechowski, J. P., Armstrong, J. P. K., & Stevens, M. M. (2020). Tailoring gelation mechanisms for advanced hydrogel applications. *Advanced Functional Materials*, *30*(42), 2002759. https://doi.org/10.1002/adfm.202002759

Oliveira, A. C., Lima, G. R. F., Klein, R. S., Souza, P. R., Vilsinski, B. H., Garcia, F. P., Nakamura, C. V., & Martins, A. F. (2021). Thermo-and pH-responsive chitosan/gellan gum hydrogels incorporated with the β-cyclodextrin/curcumin inclusion complex for efficient curcumin delivery. *Reactive and Functional Polymers*, *165*, 104955. https://doi.org/10.1016/j.reactfunctpolym.2021.104955

Oliveira, S. M., Fasolin, L. H., Vicente, A. A., Fuciños, P., & Pastrana, L. M. (2020). Printability, microstructure, and flow dynamics of phase-separated edible 3D inks. *Food Hydrocolloids*, *109*, 106120. https://doi.org/10.1016/j.foodhyd.2020.106120

Ordoñez, R., Contreras, C., González-Martínez, C., & Chiralt, A. (2021). Edible coatings controlling mass loss and Penicillium roqueforti growth during cheese ripening. *Journal of Food Engineering*, *290*, 110174. https://doi.org/10.1016/j.jfoodeng.2020.110174

Ozel, B., & Oztop, M. H. (2023). Rheology of food hydrogels, and organogels. In J. Ahmed, S. Basu (Eds.), *Advances in food rheology and Its applications*. Development in food rheology (pp. 661-688). Woodhead.

Patruni, K., & Rao, P. S. (2023). Viscoelastic behaviour, sensitivity analysis and process optimization of *aloe vera*/HM pectin mix gels: An investigation using RSM and ANN and its application to food gel formulation. *LWT – Food Science and Technology*, *176*, 114564. https://doi.org/10.1016/j.lwt.2023.114564

Rahmatpour, A., Alijani, N., & Mirkani, A. (2023). Supramolecular self-assembling hydrogel film based on a polymer blend of chitosan/partially hydrolyzed polyacrylamide for removing cationic dye from water. *Reactive and Functional Polymers*, *185*, 105537. https://doi.org/10.1016/j.reactfunctpolym.2023.105537

Saad, F., Mohamed, A. L., Mosaad, M., Othman, H. A., & Hassabo, A. G. (2021). Enhancing the rheological properties of *Aloe vera* polysaccharide gel for use as an eco-friendly thickening agent in textile printing paste. *Carbohydrate Polymer Technologies and Applications*, 2, 100132. https://doi.org/10.1016/j.carpta.2021.100132

Sempere-Ferre, F., Giménez-Santamarina, S., Roselló, J., & Santamarina, M. P. (2022). Antifungal in vitro potential of *Aloe vera* gel as postharvest treatment to maintain blueberry quality during storage. *LWT – Food Science and Technology*, *163*, 113512. https://doi.org/10.1016/j.lwt.2022.113512

Serrano-Lotina, A., Portela, R., Baeza, P., Alcolea-Rodriguez, V., Villarroel, M., & Ávila, P. (2022). Zeta potential as a tool for functional materials development. *Catalysis Today*. https://doi.org/10.1016/j.cattod.2022.08.004

Zhang, J., Wang, G., Liang, Q., Cai, W., & Zhang, Q. (2019). Rheological and microstructural properties of gelatin B/tara gum hydrogels: Effect of protein/polysaccharide ratio, pH and salt addition. *LWT – Food Science and Technology*, *103*, 108-115. https://doi.org/10.1016/j.lwt.2018.12.080

Zhang, N., Li, X., Ye, J., Yang, Y., Huang, Y., Zhang, X., & Xiao, M. (2020a). Effect of gellan gum and xanthan gum synergistic interactions and plasticizers on physical properties of plant-based enteric polymer films. *Polymers*, *12*(1), 121. https://doi.org/10.3390/polym12010121

Zhang, W. H., Wu, J., Weng, L., Zhang, H., Zhang, J., & Wu, A. (2020b). An improved phenol-sulfuric acid method for the determination of carbohydrates in the presence of persulfate. *Carbohydrate Polymers*, *227*, 115332. https://doi.org/10.1016/j.carbpol.2019.115332